Chapter 2

InGaP/GaAs Heterostructure Grown by LP-MOCVD

In this chapter, order-disorder InGaP/GaAs heterostructures grown by LP-MOCVD was characterized with double crystal X-ray diffraction (DCXRD), scanning electron microscopy (SEM), Raman scattering spectra and photoluminescence (PL) measurement. Optical and structural properties of InGaP/GaAs heterostructures are investigated as a function of growth temperature.

2.1 Introduction to LP-MOCVD System

Metallorganic chemical vapour deposition (MOCVD) is a unique and important epitaxial crystal growth technique, which uses the group III alkyls and the group V hydrides as source materials in a quartz tube that contains carbon susceptor. The technique was pioneered by Manasevit in 1986 who demonstrated that TMGa (Trimethylgallium) mixed with AsH_3 (arsine), which pyrolyzed at temperatures between 600 and 700℃ in an H_2 atmosphere was able to grow thin single crystals of GaAs on GaAs substrate. MOCVD can grow heterostructures, multiquantum wells (MQW) and superlattices (SL) with fast gas-switching in composition as well as in doping profiles in crystal growth by fast changes of the gas composition in the chamber.[1] In comparison with other growth methods, MOCVD has the advantages: (1) reduction of auto-doping and out-diffusion; (2) elimination of parasitic nucleations in the gas phase; (3) improvement of the impurity profiles and interface sharpness; (4) elimination of memory effect.[2]

2.1.1 LP-MOCVD System

a. Gas handling system

The gas handling system includes (1) hydrogen purifier (2) thermal bath (3) mass flow controllers (4) manifold.

(1) High-purity hydrogen is necessary for epitaxy growth to prevent epitaxial layers from unexpected contamination. It consists of palladium as a diffusion medium for impure hydrogen molecules.

(2) Metallorganic sources are usually stored in stainless steel cylinders. The partial pressure of the source vapor is regulated by precisely controlling the temperature of the metallorganic source bubbler. Thermal bath could control the temperatures from -30 to 100℃ and should be kept at a constant temperature to meet the stable growth condition during epitaxy.

(3) Mass flow controller is used to accurately control the mass flow rate of starting materials.

(4) Before gas sources introduce into the reactor chamber, a manifold which is clean and leak free is used to determine whether the sources should enter the reactor or bypass into the exhaust system.

b. Reactor chamber

There are two basic reactor designs in MOCVD system. Manasevit and Simpson[3] developed a vertical design, which the gas flow is perpendicular to the substrate surface, and Bass[4] developed a horizontal reaction chamber, which the gas flow is parallel to the substrate surface. The reactor which used in this thesis is a horizontal type. The presence of vortices and dead volumes (sharp corners in reactor inlet) will

act as sources of unwanted materials that are hard to completely remove and will cause the memory effect. Therefore, the smoothness of the reactor shape is very important and a well-designed reactor can eliminate the memory effect.

c. Heating system for pyrolysis temperature

In this study, graphite susceptor is heated by RF heating system which is inductively coupled to the RF coil. In addition, R-type thermocouple is used to measure the susceptor temperature.

d. Exhaust system and safety apparatus

Exhaust system serves to remove unwanted gases from the reaction chamber and provide a path for reactants to bypass the reaction zone. The toxic gas monitor system can be used to detect the toxic gases. It provides an instantaneous readout of gas concentration whenever the concentration of a particular gas exceeds the pre-set level.

Figure 2.1 depicts a schematic diagram of an MOCVD reactor and tube cross section.

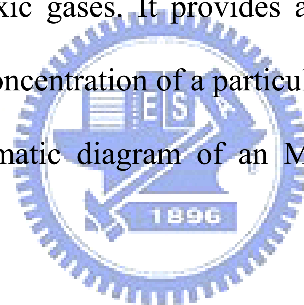

2.2 MOCVD Epitaxial Theory of InGaP/GaAs Heterostructure

The MOCVD growth theory is generally subdivided into two parts, thermodynamics and kinetics component. Thermodynamics determine the driving forces of the overall growth process, and it can define as the rates of each reaction step during epitaxy process. In addition, it is necessary to know how to control the transport rate of the reactants to the vapor/solid interface layer for epitaxial growth. The hydrodynamics and mass transport theory should be modeled for the growth process.

2.2.1 Starting materials

a. Triethylgallium

Triethygallium (TEGa) is marginally stable. TEGa reacts with the hydrides at high growth temperatures in atmosphere-pressure reactor, resulting in depletion of the reactants from the vapor. This produces low growth rates and large thickness nonuniformities in the direction of the gas flow. However, in reduced pressure reactors, the use of TEGa is found to reduce the carbon concentrations significantly in GaAs, this is because TEGa pyrolyzes without producing the CH_3 radicals which is the main source of carbon in the epitaxial layers. The pyrolysis curves of TEGa are shown in Figure 2.2.

b. Trimethylindium

Trimethylindium (TMIn) kept at a 15℃ thermal bath presents as a solid phase because its melting point is 88℃. To avoid the unstable vapor pressure of TMIn, increasing the surface area by breaking it into small pellets is necessary. TMIn can be decomposited fully at 350℃ in hydrogen ambient. The results of TMIn decomposition studied in three different carrier gases, H_2, D_2 and He, are shown in Figure 2.3

c. Arsine and phosphine

The chemical sources used for Ⅲ-Ⅴ epitaxial growth techniques are most often highly toxic or flammable. In particular, the hydrides such as arsine (AsH_3) and phosphine (PH_3) are highly toxic with threshold level values (TLV) of 0.05 and 0.3, respectively. Group Ⅴ hydrides, however, are widely used in MOCVD epitaxy process owing to their lower cost and better controlled epitaxy quality than organometallic group Ⅴ sources. Larsen *et al.*[5] studied AsH_3 pyrolysis in a quartz MOCVD reactor using a D_2 carrier gas as well as in N_2 carrier gas to label the

products for mass spectrometric analyses, as shown in Fig. 2.4. The temperature at which pyrolysis is 50% complete, T50, for a residence time of 4s, was found to be approximately 600℃ on SiO_2 surface independent of the ambient.

In contrast to TEGa and TMIn, PH_3 is considerately hard to pyrolyze. Its decomposition is less than 10% at 700℃, , so high Ⅲ/V ratio is utilized during the growth of InGaP epitaxy process. Moreover, the InP is able to increase the pyrolysis of PH_3 up to 50% at 525℃. The PH3 pyrolysis curves are shown in Figure 2.5. In this thesis, triethylgallium (TEGa), trimethylindium (TMIn), phosphine (PH_3), and arsine (AsH_3) were used as precursors. The physical properties of these materials are listed in Table 2-1.

2.2.2 Precursor properties

The precursor properties such as saturation vapor pressure and molar flow rate should be considered clearly before the crystal growth. An important relation known as the Clausius-Clapeyron equation, which gives the slope of the vapor pressure curve must be discussed.

$$LogP = A - B / T$$

where P is the vapor pressure, A,B are the known constants, and T is absolute temperature. A high purity hydrogen gas was used to carry the precursors. The approximate evaluation of the molar rate (Fm) can be calculated with the following equation.

$$Fm\left(mole / \min\right) = \frac{P\left(torr\right)}{760\left(torr\right)} \times \frac{F_v\left(sccm\right)}{22400\left(c.c.\right)}$$

where P is the vapor pressure of reactant, and *Fv* is the flow rate of hydrogen.

2.2.3 Thermodynamics

Thermodynamics determines the driving force of each step during MOCVD epitaxy process and predicts whether epitaxial reactions would occur or not. Furthermore, the growth rate for an epitaxy process can also be estimated from thermodynamic calculations. In addition, thermodynamics is also useful in establishing the phase diagram of a multi-component system by calculating the energies of the solid for different temperatures and pressures.

2.2.4 Kinetics

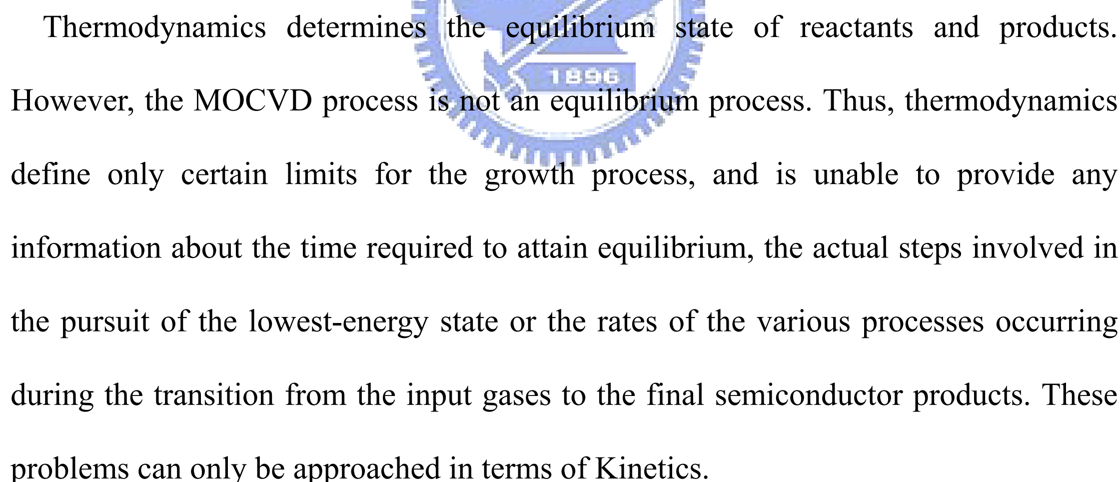

Thermodynamics determines the equilibrium state of reactants and products. However, the MOCVD process is not an equilibrium process. Thus, thermodynamics define only certain limits for the growth process, and is unable to provide any information about the time required to attain equilibrium, the actual steps involved in the pursuit of the lowest-energy state or the rates of the various processes occurring during the transition from the input gases to the final semiconductor products. These problems can only be approached in terms of Kinetics.

2.2.5 Hydrodynamics and mass transport

In hydrodynamics of MOCVD epitaxy, the reactor design and system pressure are most important. A well-designed reactor can eliminate the thermal convections and

other disturbances, and improves the uniformity of the epitaxial layer. Reducing reactor pressure increases the gas flow rate and decreases the thickness of the boundary layer. Moreover, the low-pressure MOCVD system also significantly decreases the pyrolysis rate of the reactants in the vapor phase.

When growth rate is limited by the mass transport, the flux of group Ⅲ reactant can be expressed as follows:

$$J = \frac{D(P_0 - P_i)}{RTd_0}$$

D: diffusion coefficient

Po: group Ⅲ reactant partial pressure in vapor phase

Pi: group Ⅲ reactant partial pressure in substrate interface

do: thickness boundary layer

At the same time, when surface reaction rate is larger than mass transport rate, $Pi \ll Po$, hence, growth rate is proportional to the gas flow(or partial pressure) of group Ⅲ reactants.

2.2.6 Growth rate control Mechanism

The growth rate in MOCVD epitaxy process is usually lower than expected from thermodynamic calculations. This is due to the surface reaction rate controlled by kinetics and mass transport of reactants in vapor phase is not fast enough, the whole system can't reach the thermal equilibrium state. The growth rate depends on the slowest reaction step. The relation between growth temperature and growth rate can be subdivided into the three regions. Figure 2.7 shows experimental results of this

phenomenon.

a. Kinetically controlled region

At low temperature, the surface adsorption rate of reactant source is lower than the diffusion rate of reactant source in the boundary layer. Therefore, in this region, the growth rate depends on the surface reaction rate and increases with increasing temperature.

b. Mass-transport-limited region

At intermediate temperature, the surface adsorption rate of the reactant source is much higher than the diffusion rate of the reactant source in the boundary layer. Therefore, in this region, the growth rate depends on the reactant diffusion rate and is independent of the growth temperature.

c. Thermodynamically controlled region

At high temperature, the adsorption rate of the surface atom increases; meanwhile, the parasitic reactions occurred in vapor phase cause the depletion of the reactant source. Thus, the growth rate decreases with increasing temperature in this region.

2.2.7 The growth parameters for the growth of InGaP/GaAs material system

The qualities of epi-layers are affected extremely by the epitaxy growth parameters such as growth temperature (*Tg*), growth pressure, Ⅴ/Ⅲ ratio and Ⅲ/Ⅲ ratio (if in InGaP ternary compound system). In this study, the growth pressure is kept at 40 torr. The other growth parameters are introduced as following.

a. Growth temperature

Growth temperature (*Tg*) is the most important parameter in the growth of InGaP

material system, however, the most proper *Tg* differs with different MOCVD systems. Most literatures reported that the *Tg* of $In_{0.5}Ga_{0.5}P$ is among 600~750℃. If *Tg* is lower, the alloy is easy to have 3-dimension growth and poor surface morphology. If *Tg* is higher, the alloy is easy to have high carbon incorporation. In this study, the InGaP/GaAs heterostructure was grown at different *Tg* from 550℃ to 750℃ to find out the most proper growth temperature. Ordering and disordering phenomea of InGaP were observed during different growth temperatures.

b. Ⅴ/Ⅲ ratio and Ⅲ/Ⅲ ratio

The input Ⅴ/Ⅲ ratio has a major effect on the incorporation of residual impurities. Because only the group Ⅴ elements are volatile at normal growth temperatures, the Ⅴ/Ⅲ ratio is typically ＞3. If Ⅴ/Ⅲ ratio isn't large enough, it will result in extremely poor surface morphologies. It is caused by the existence of group Ⅴ vacancies, furthermore, residual Ga atoms will react with P atoms to form unexpected GaP. Optimal Ⅴ/Ⅲ ratio should be determined to ensure the quality of GaAs and InGaP epi-layers. Generally, the Ⅴ/Ⅲ ratio is obtained from:

Ⅴ/Ⅲ＝[Hydride]/[Alkyl]

In InGaP ternary material system, the Ga/In ratio also plays a significant role in controlling the qualities of the epi-layers. Only by precisely controlling the ratio between Ga and In, the growth of the lattice-matched InGaP/GaAs epi-layer is possible. Yuan *et al.*[6] reported that the lattice constant misfit between InGaP and GaAs, ｜Δa/a｜, should be lower than 0.1% ,so that the mirror-like surface of epitaxy can be obtained.

2.2.8 Disordered and ordered $In_{0.49}Ga_{0.51}P$ structure

$In_{0.49}Ga_{0.51}P$ (hereafter written as InGaP) layers grown by MOCVD, in generally, form the Cu-Pt ordered structure.[7-11] The Cu-Pt structure with ordering on the {111} planes which Ga and In atoms spontaneously divide into alternating {111} monolayers during growth rather than forming an random disorder structure. A disorder structure which the Ga and In atoms randomly distributed on the group Ⅲ sublattice is strongly influenced by growth conditions such as growth temperature, growth rate, Ⅴ/Ⅲ flux ratios.[9,12] In this study, structural transformation induced by different growth temperatures was characterized. Controlling the growth temperature can cause variations in the group Ⅲ sublattice distributions and different atomic arrangement changes the band structure of the crystal. The degree of ordering has significant influence on energy band gap of InGaP.[13] It is well known that the band gap of InGaP measured by low temperature PL can be used to characterize the degree of atomic ordering, i.e. η. Atomic ordering (η) can be calculated using the equation[14] $\eta = [(2005 - E_{PL})/471]^{1/2}$, where E_{PL} (meV) is the PL peak energy at low temperature. According to this equation, the ordering parameter η is lower if the band gap is larger (more disorder). Disorder InGaP interface has type I band alignment (straddle) and will tranform from type I to type II (stagger) as the InGaP becomes more ordered. Figure 2.6 shows the Cu-Pt type ordered structure of InGaP.[15] On the other hand, disordered InGaP has a Zinkblende structure. Microstructure evolution of ordering effect of InGaP has also been developed by Raman scattering spectra.[16,17] Raman scattering spectra can detect the wavelength of a small fraction of the radiation scattered by molecules differs from those of the incident beam. Therefore, the shifts in wavelength by scattering depend on the order/disorder structure of the molecules.

2.3 Experimental procedures

All of the InGaP/GaAs heterostructures used in this study were grown on undoped GaAs (100) substrates. Each crystal growth was performed in a horizontal flow reactor and the chamber pressure was kept 40 Torr by throttle valve. TEGa and TMIn were used as group III precursors and AsH_3 and PH_3 were used as group V precursors. The growth rates were 1.5 μm/hr and 1.52 μm/hr for InGaP and GaAs respectively. First, InGaP/GaAs heterointerface was optimized by fast gas-switching method.[18] After the growth of the GaAs buffer layer, the group III precursor is switched off and an AsH_3 overpressure is maintained for 20 seconds. Then, PH_3 is introduced for 5 seconds before the group III precursors are introduced. A similar recipe is used for the InGaP-to-GaAs interface. However, due to the substitution of P by As is more efficient than GaAs-to-InGaP, AsH_3 overpressure should be avoided. Quantum well structures were grown for the characterization of the InGaP/GaAs heterointerfaces. Double crystal X-ray diffraction (DCXRD), scanning electron microscopy (SEM), and photoluminescence (PL) measurement were used to identify the interfacial abruptness. Second, the temperature dependences of energy band gap and Raman modes on order-disorder InGaP are discussed.

2.4 Results and discussion

2.4.1 Characterizations of the InGaP/GaAs heterointerfaces

Double crystal X-ray diffraction (DCXRD) was used to identify the information on lattice mismatch, interfacial quality and layer composition of the InGaP/GaAs heterostructures. Figure 2.7 shows the DCXRD patterns of bulk InGaP layer grown on

GaAs substrate at 650℃. The DCXRD data show a sharp InGaP peak and the lattice mismatch is lower than 1000 ppm, suggesting that abrupt interface was formed between InGaP and GaAs. Additional evidence showing the abruptness of the InGaP/GaAs heterostructures can be seen from the room temperature photoluminescence (PL) measurement, as shown in Fig. 2.8. As can be seen from this figure, the full width half maximum (FWHM) of the proposed heterostructure was 18.8 nm and the energy band gap was 1.85 eV, indicating that the interface was very sharp. Fast gas-switching method was used to improve the interface between GaAs and InGaP layer. During the growth of the InGaP/GaAs QWs by MOCVD, the group III precursor is switched off and an AsH_3 overpressure is maintained for 20 seconds. Then, PH3 is introduced for 5 seconds before the group III precursors are introduced. For the InGaP-to-GaAs interface, however, AsH3 overpressure should be avoided. If the substitutions of P atoms by As atoms were very serious, it will cause the interface to be very rough owing to the formation of InGaAsP, as shown in Fig. 2.9. Figure 2.10 shows cross-section of the InGaP/GaAs QW with the optimized switching as observed by SEM. As can be seen from this figure, after optimizing the gas switching of the GaAs and the InGaP during growth, high quality InGaAs/GaAs heterointerfaces with abrupt interfaces can be achieved.

2.4.2 Photoluminescence and Raman study of ordered and disordered InGaP

Figure 2.11 shows PL spectra for the InGaP layers grown on GaAs at 650 and 700 ℃, respectively. It is clear that the emission energy of 700℃-grown InGaP is shifted to a shorter wavelength (blue shift). The optical band gap increases as the growth

temperature was increased from 650 to 700℃, indicating that the InGaP sample grown at 700℃ contains a relatively high degree of atomic disorder. Figure 2.12 shows the changes in the InGaP (Eg) with grown temperature measured by room temperature PL. Under a fixed InGaP composition, a high band gap of 1.93 eV corresponding to a random (disorder) distribution of Ga and In on the group III sublattice was observed at the growth temperature of 730℃. On the other hand, a low band gap of 1.83 eV corresponding to an atomically ordered distribution was grown at 630℃. The difference of the band gap in InGaP can vary as much as 100meV depending on the growth condition. It is well known that the lower ordering η results in larger band gap. Therefore, it is important to control the ordering of InGaP for advanced electronic devices applications such as HBTs. The disordered InGaP has a larger energy band gap and ΔE_v, is expected that the HBTs using disordered InGaP as emitter material could block the hole back-injection and get better current gains for the device than when the ordered InGaP emitter is used.

In addition to photoluminescence, Raman scattering spectra was used to investigate a possible ordering of the In and Ga atoms in the group III sublattice. Figure 2.13 shows the Raman scattering spectra of the samples grown at 620 and 730℃. Bedel et al.[19] reported that the fitted values of GaP-like LO, InP-like LO, and TO phonon mode behavior of InGaP measured by Raman spectra. The fitted values are

$\omega_{LO}(GaP)= 404.99-38.97x-18.18x^2$ (cm-1), where x= mole fraction of In

$\omega_{LO}(InP)= 394.59-80.36x+30.26\,x^2$ (cm-1)

$\omega_{TO}= 368.82-88.59x+26.04\,x^2$ (cm-1)

Jusserand and Slempkes[20] have also reported that the Raman peak at about $380cm^{-1}$ is marked as GaP-like longitudinal-optical (LO) mode, while the peak at

$360 cm^{-1}$ as the InP-like LO mode by a two-mode model. The weaker signal at about $330 cm^{-1}$ is attributed to the transverse-optical (TO) phonons which is forbidden in the ordered InGaP. It can be concluded that the InGaP grown at 730℃ exhibits a more disordered characteristic than the sample grown at 620℃.

2.5 Conclusions

The effect of group V switching time on the improvement of the interfacial layers in the InGaP/GaAs heterostructures grown by MOCVD has been studied. By using fast gas switching method, sharp interfaces can be achieved in the InGaP/GaAs heterostructures as judged by the DCXRD, PL, and SEM analysis data. The dependence of the band gap of InGaP material with different growth temperatures are characterized by room temperature PL measurement. Under a fixed InGaP composition, a high band gap of 1.93 eV can be achieved at 730℃, showing a more disorder characteristic. However, a low band gap of 1.83 eV corresponding to an atomically ordered distribution was obtained at 630℃. Raman spectra analysis also shows that the InGaP grown at 730℃ exhibits a more disordered characteristic by considering a two-mode model. It exhibits a transverse-optical (TO) phonon mode which is forbidden for the ordered InGaP grown at 620℃.

2.6 References

1) M Razeghi: *The MOCVD Challenge Volume 1* (Adam Hilger, Bristol, 1989) p.9.

2) C. Y. Chang, Y. K. Su, M. K. Lee, L. G.. Chen and M. P. Houng: J. Cryst. Growth **5** (1981) 24.

3) Manasevit H M and Simpson W I: J. Electrochem. Soc. **118** (1971) C291.

4) Bass S J: J. Cryst. Growth **31** (1975) 172.

5) C. A. Larsen, N. I. Buchan and G. B. Stringfellow: Appl. Phys. Lett. **52** (1988) 480.

6) J. S. Yuan, M. T. Tsai, C. H. Chen, R. M. Cohen and G. B. Stringfellow: J. Appl. Phys., **60** (1986) 1346.

7) Soon Fatt Yoon, Kia Woon Mah and Hai Qun Zheng: Jpn. J. Appl. Phys. **38** (1999) 5740.

8) G. B. Stringfellow and L. C. Su: Appl. Phys. Lett. **66** (1995) 3155.

9) O. Ueda, M. Takikawa, J. Komeno and I. Umebu: Jpn. J. Appl. Phys. 26 (1987) L1824.

10) G. B. Stringfellow and G. S. Chen: J. Vac. Sci. Technol. **B9** (1991) 2182.

11) A. G. Norman, T. Y. Seong, B. A. Phillips, G. R. Booker and S. Mahajan: Inst. Phys. Conf. Ser. **134** (1993) 279.

12) A. Gomyo, T. Suzuki, K. Kobayashi, S. Kawata and I. Hino: Appl. Phys. Lett. **50** (1987) 673.

13) C. Nozaki, Y. Ohba, H. Sugawara, S. Yasuami and T. Nakanisi: J. Cryst. Growth **93** (1988) 406.

14) J. D. Song, J. M. Kim and Y. T. Lee: Appl. Phys. A **72** (2001) 625

15) L. Gonzalez, Y. Gonzalez and M. L. Dotor: Appl. Phys. Lett. **72** (1998) 2595.

16) M. Zachau and W. T. Masselink: Appl. Phys. Lett. **60** (1992) 2098.

17) H. Lee, D. Biswas, M. V. Klein, H. Morkoc, D. E. Aspnes, B. D. Choe, J. Kim and C. O. Griffiths: J. Appl. Phys. **75** (1994) 5040.

18) Q. Yang, Q. J. Hartmann, A. P. Curtis, C. Lin, D. A. Ahmari, D. Scott, H. C. Kuo, H. Chen and G. E. Stillman: IEEE (1998) 95.

19) E. Bedel, R. Carles, G. Landa, and J. B. Renucci: Rev. Phys. Appl. **19** (1984) 17

20) B. Jusserand, and S. Slempkes: Solid State Commun. **49** (1984) 95.

Precursor	Formula	Melting point (℃)	boiling point (℃)	Vapor pressure(Torr)
TEGa	$(C_2H_5)_3Ga$	-82.3	142.6	3.75 at 15 ℃
TMIn	$(CH_3)_3In$	88	135.8	1.15 at 15 ℃
Arsine	AsH_3	-	-62.5	760 (room temp.)
Phosphine	PH_3	-	-87.7	760 (room temp.)

Table 2.1 Properties of the starting materials

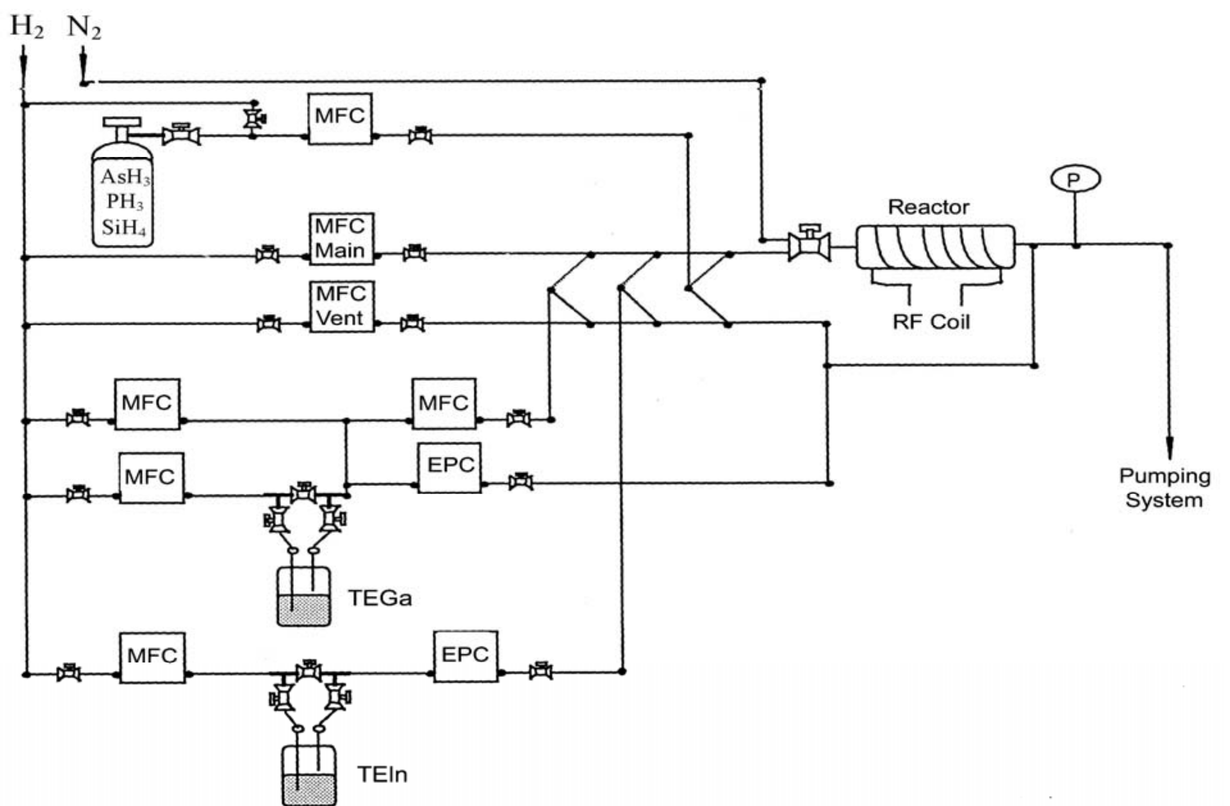

Fig 2.1. Schematic diagram of an MOCVD reactor and tube cross section.

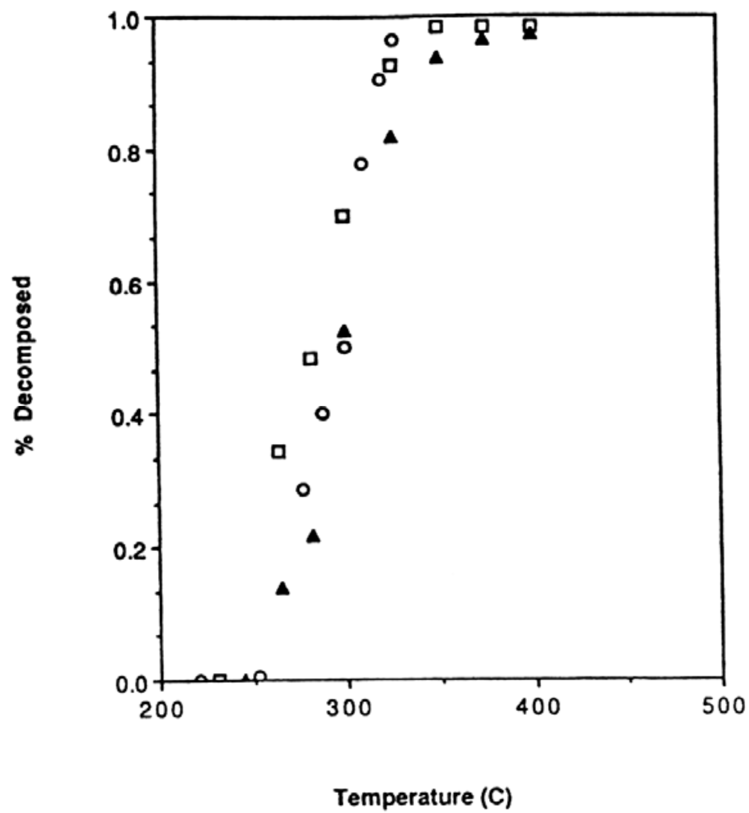

Figure 2.2 The pyrolysis curves of TEGa

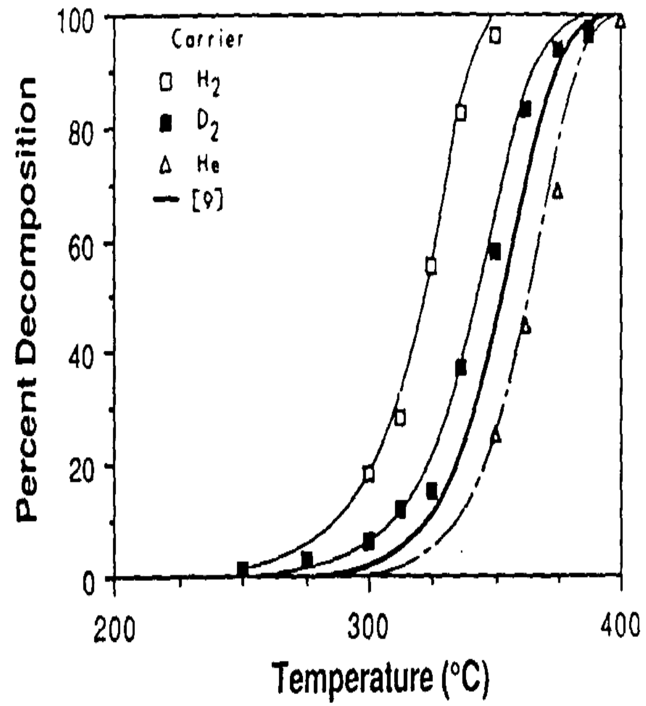

Figure 2.3 TMIn decomposition ratio in three different carriers,H_2,D_2 and He

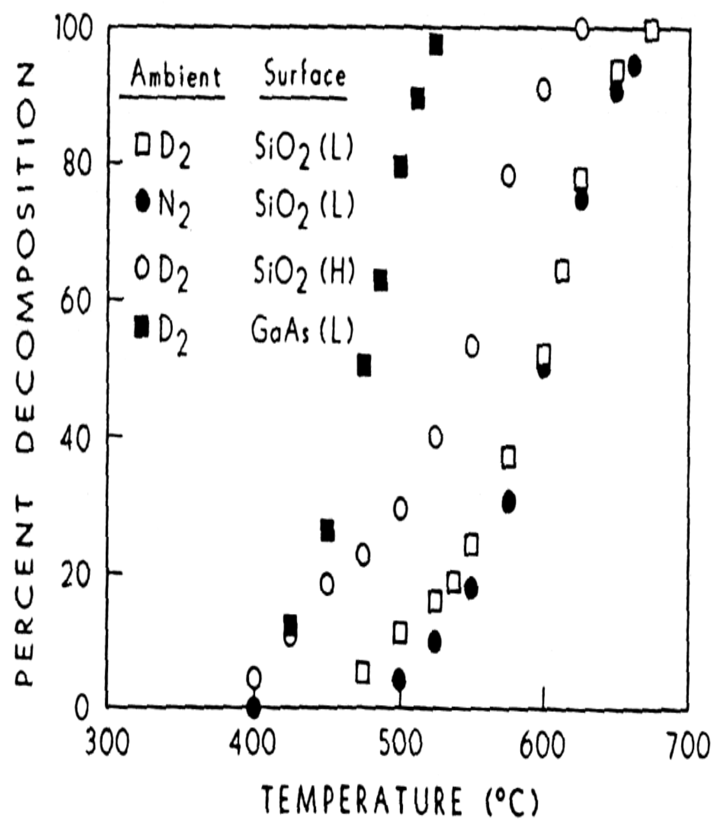

Figure 2.4 The pyrolysis curves of AsH_3

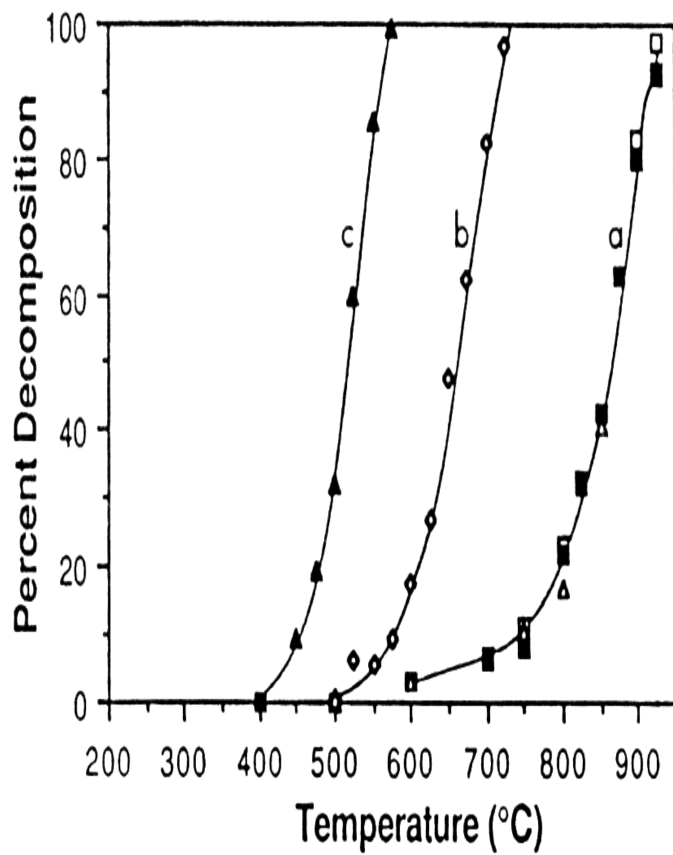

Figure 2.5 The pyrolysis curves of PH_3

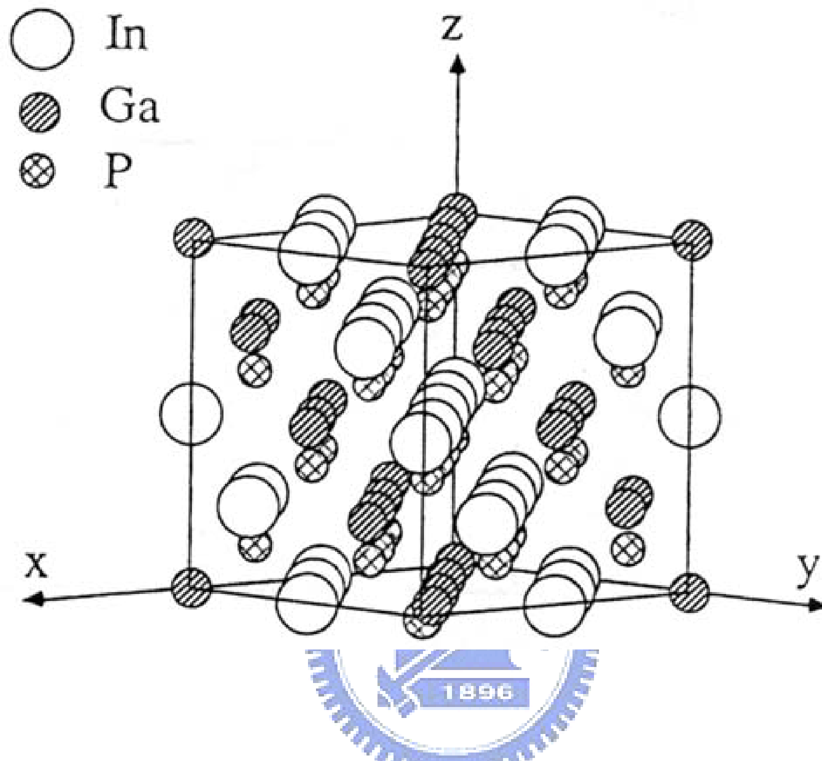

1896

Fig 2.6 The Cu-Pt type ordered structure of InGaP

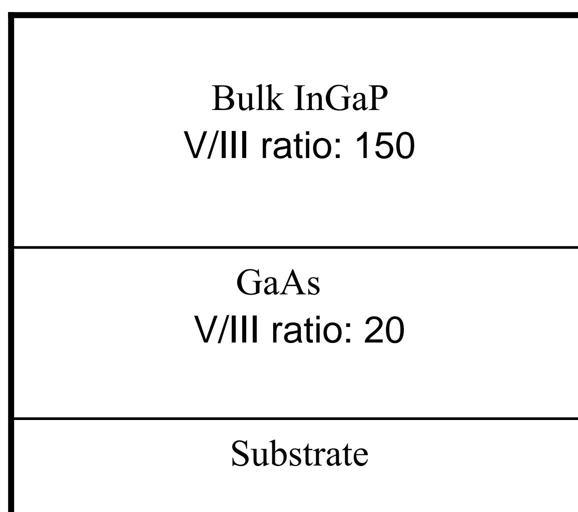

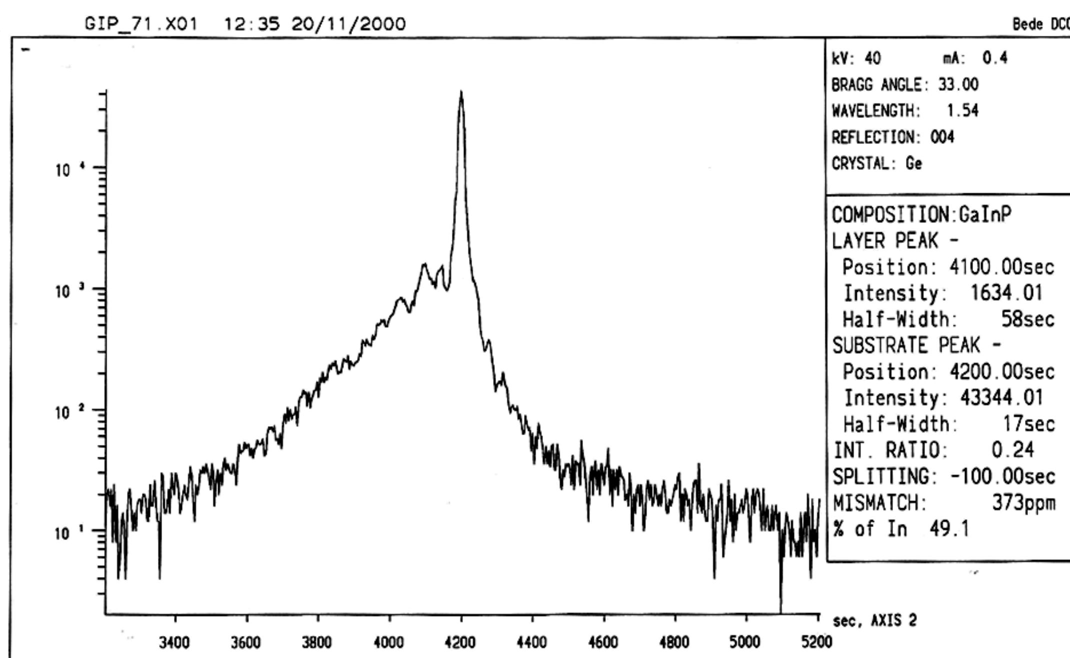

Figure 2.7 A (400) double crystal rocking curve for a 0.5μm thick InGaP layer grown on a (100) oriented substrate at 650℃.

Eg(eV)	FWHM(nm)
1.85	18.8

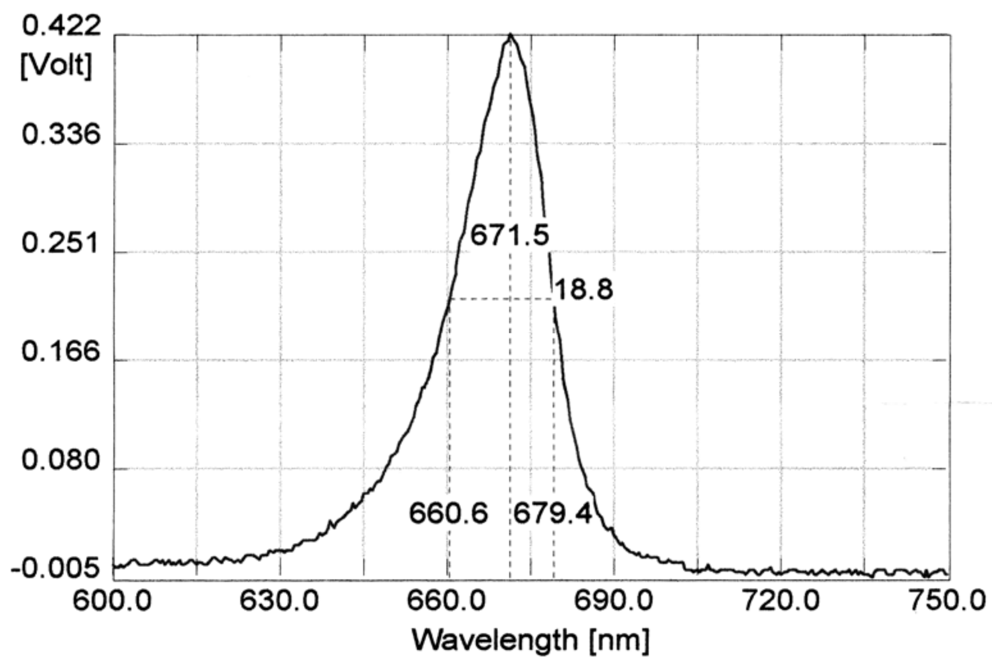

Figure 2.8 Room temperature photoluminescence spectrum of the InGaP layer on GaAs substrate grown at 650℃ by LP-MOCVD (V/III=150).

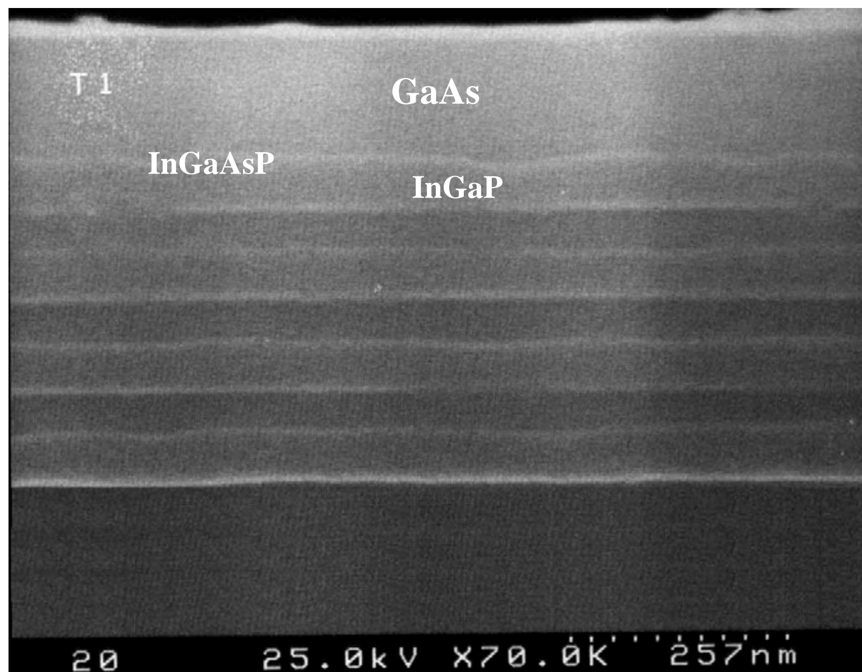

Figure 2.9 Cross-sectional SEM image of InGaP/GaAs QWs. The rough interfaces was due to the formation of InGaAsP.

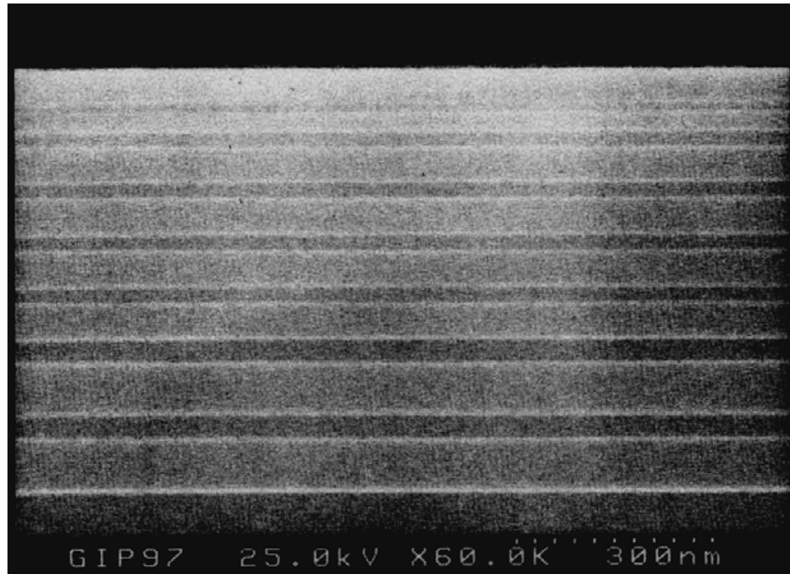

Figure 2.10 Cross-sectional SEM image of InGaP/GaAs QWs with the optimized switching sequence.

1896

(a)

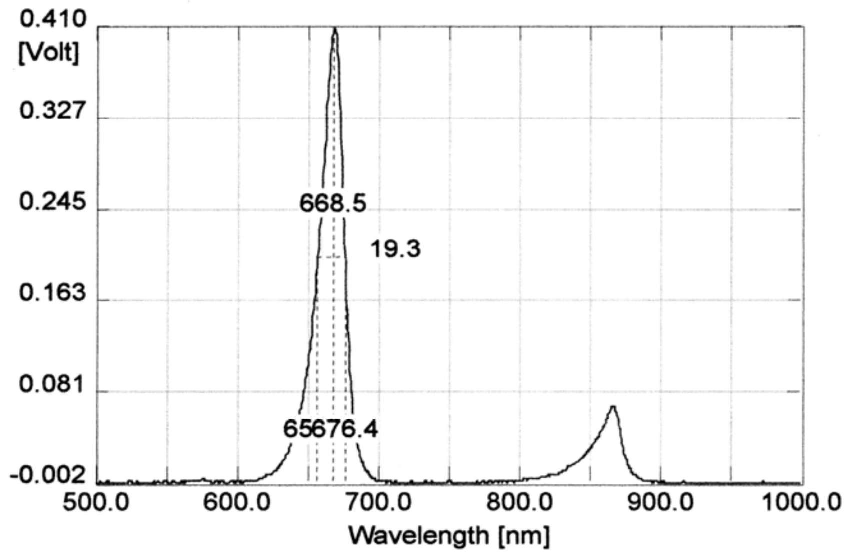

(b)

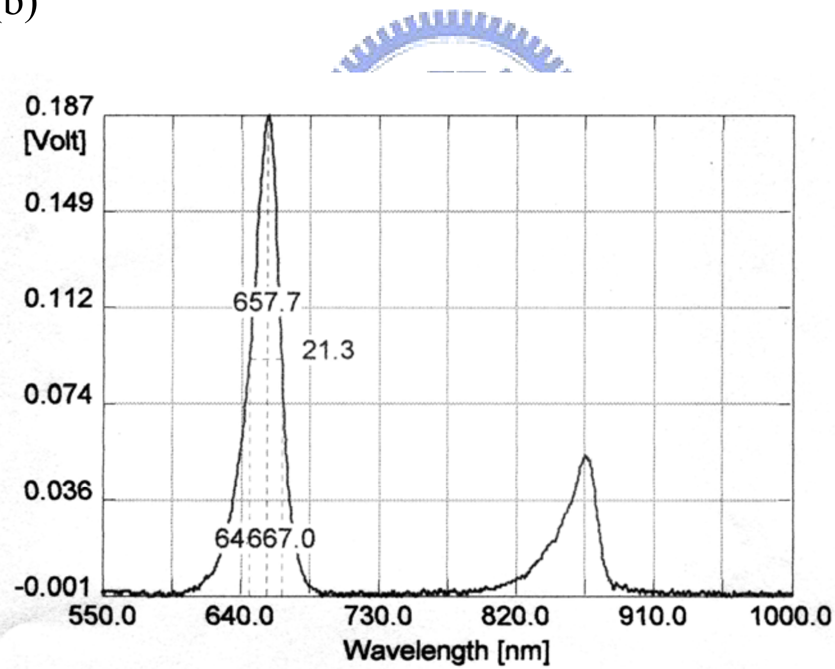

Figure 2.11 PL spectra of (a) ordered InGaP grown at 650℃ and (b) disordered InGaP grown at 700℃

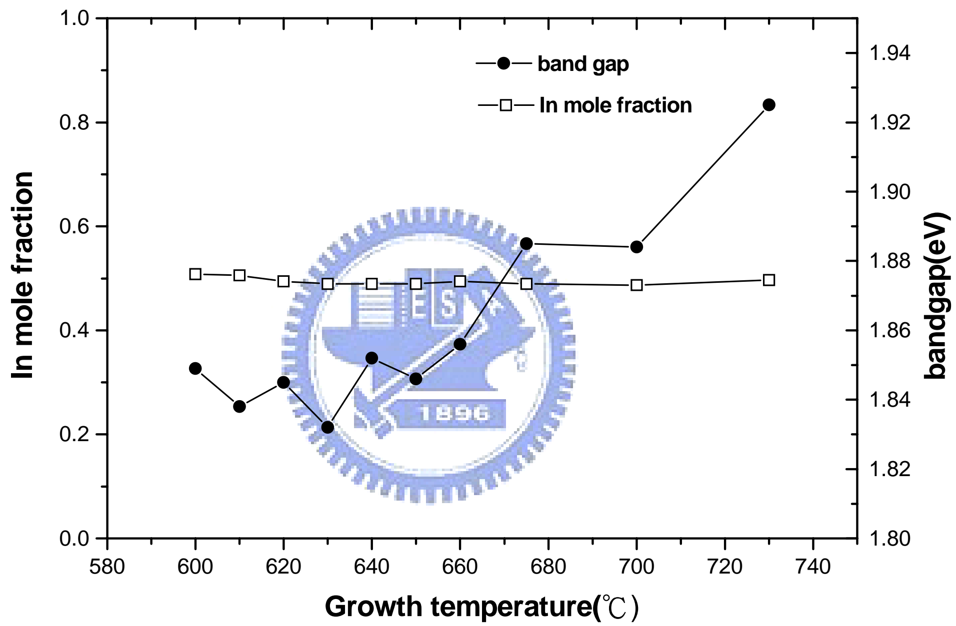

Figure 2.12 Changes in the InGaP energy gap with growth temperature as measured by room temperature PL. The In mole fraction was kept constant.

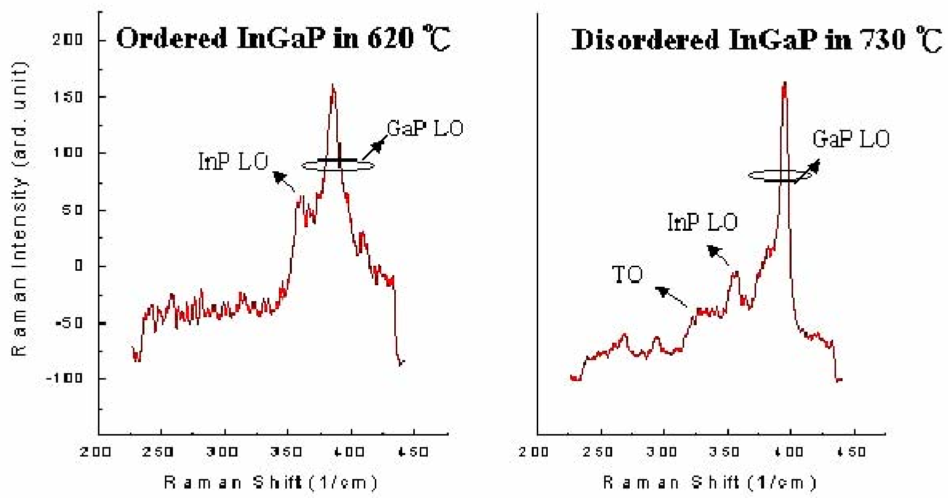

Figure 2.13 Raman spectra for InGaP grown at 620 ℃and 730℃.